

MultiShape Theory

The code library 2DChebClass, introduced in [1], is a tool for solving PDEs using pseudospectral methods in one and two dimensions on different domains, such as quadrilaterals, wedges and periodic boxes. The aim of this library is to provide a toolbox for solving PDEs in an efficient and user-friendly manner. This includes the automatic set-up of differentiation and convolution matrices, interpolation and integration vectors, as well as domain discretization using pseudospectral methods, identification of boundaries and application of boundary conditions. PDEs can be solved on various domains, which all have in common that they can be mapped conformally to a unit square $[-1, 1]^2$, the computational domain. Examples of this include rectangles, quadrilaterals, wedges in polar coordinates and periodic domains. All computations are done on this computational domain and mapped back to the specific shape of interest. The library's features are thoroughly explained in [1].

While the library supports solutions to PDEs on various single shapes, the method is now extended to compute the solution to a PDE on a complex domain, or multishape, which is composed of a number of quadrilaterals and wedges. The philosophy of this multishape code is to use the existing code library [1], which is designed to efficiently and accurately solve PDEs on individual shapes, to do the same on a multishape with minimal additional effort for the user.

+++ Explain that multishape is composed into elements before explaining SEM +++ The solution of a PDE on such a multishape domain is achieved by employing the spectral element method (SEM), by thinking of each of the shapes as the discretization elements of SEM. This method is similar in spirit to the finite element method (FEM). FEM discretizes a domain into elements and computes the solution to a given PDE on each of those elements. Expansions of basis functions are used, which are low order polynomials, for interpolation on an equispaced grid. SEM follows the same philosophy but uses higher order basis functions such as Chebyshev or Lagrange polynomials and Chebyshev-Lobatto points on the interpolation grid (++ comp or phys? +++) on each element, as opposed to an equispaced grid, to avoid the Runge phenomenon. At the intersections between the elements, C^0 continuity is enforced. SEM was first introduced by Patera [2] using Chebyshev polynomials as basis functions and later adapted to Lagrange polynomials by Komatitsch and Vilotte [3]. While this method is widely used to solve PDEs in their weak form, in this work the strong form of the PDE is considered, since this aligns best with the existing framework. (!) Furthermore, instead of just requiring continuity of the solution at the intersection of two elements, the flux (or first derivatives) are also matched. +++ say that this is because we need two matching conditions and why +++

In the multishape extension to 2DChebClass, a given PDE is solved on each shape individ-

ually (+++ subject to external and matching BCs +++), using the preexisting tools in the code library. This is done simultaneously by stacking the differentiation matrices, integration and interpolation vectors for each shape on top of one another. The initial condition is also given as a stacked vector, containing the information for each shape. This stacking is done using a fixed order of the shapes specified by the user. For example, given a function f on a domain Ω consisting of three shapes labeled 1, 2, 3, the solutions on each shape f_1 , f_2 and f_3 are stored as (+++rewrite so they look like they are stacked vertically+++):

$$f_{\Omega} = [f_1|f_2|f_3],$$

and similarly, a differentiation matrix D_{Ω} is defined as:

$$D_{\Omega} = [D_1|D_2|D_3],$$

where the D_i , $i = 1, 2, 3$ are the differentiation matrices on each shape.

The code automatically identifies the intersection boundaries between two shapes when setting up the multishape. The code loops through each face of each shape and compares the points of each face with all faces of the other shapes. It furthermore checks for the possibility that the points of two faces are the same but in reverse order. ++mention small errors due to maps eg polar to quadrilateral etc ++

Once the intersections between the neighboring shapes are identified, user defined boundary conditions can be applied. There are currently two options, although the addition of further boundary conditions is straightforward. For a continuous (++ more than cts ++) solution on the multishape, both the solution to the PDE and the flux are matched at these intersection boundaries. Alternatively, hard walls between two shapes can be simulated easily, by applying a no-flux boundary condition at that intersection boundary. On boundaries which are on the outside of the multishape, different boundary conditions (++ i.e. the original ones from the PDE ++), such as no-flux and Dirichlet conditions, can be applied in the same way as for single shapes.

When external no-flux boundary conditions are applied, a further subtlety is that information about the normal vectors to each outward boundary need to be computed. The existing code library already provides the set of normals for each shape. The multishape extension uses this, alongside the information of which boundaries of each shape are outward boundaries, and which intersect with other shapes, to find the outward normals of the multishape. The only part that needs to be treated with care are the points where two shapes intersect at an outward boundary, since these have two different normals at that intersection point. This is treated in the same way as corners of a single shape, by taking the average of the two normals given by the two faces that meet at the given corner. This is illustrated in Figure 1.

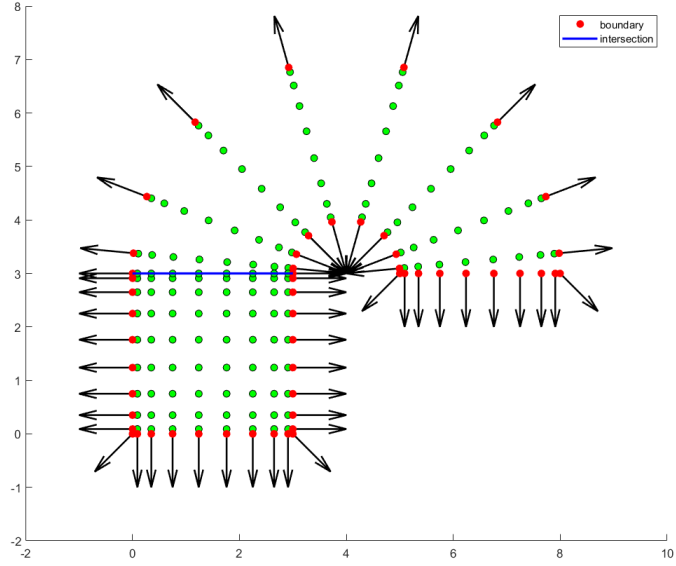


Figure 1: Normals for Multishape

The final aspect to be considered is the convolution matrix, which is needed to compute convolution integrals. It is computed in a similarly straightforward way, but since convolution is a global operation, it is not as simple as stacking the convolution matrices for the individual shapes, as is done for differentiation, integration and interpolation. The convolution integral is defined as:

$$(n \star \chi)(y) = \int \chi(y - \tilde{y})n(\tilde{y})d\tilde{y}.$$

As explained in [1] in detail, χ at $y - \tilde{y}$ is evaluated for all points in the multishape domain and transformed into a matrix $\text{diag}(\chi)$. This is integrated, using the stacked integration vector, to result in the convolution matrix, which can then be applied to a density n . +++ explain in more detail +++

1 Validation Tests

1.1 Exact Tests

Several examples are run, using exact solutions, to validate the multishape code. This is done using an exact solution to the advection diffusion equation on an infinite domain, so that Dirichlet boundary conditions, matching the value of the exact solution on the boundary of the

Table 1: Errors compared to exact solution for different discretizations (into one, two and three shapes) of the box and a quadrilateral

	One Shape	Two Shapes	Three Shapes	Four Shapes	Quadrilateral
Abs. E., $N = 20$	2.2063×10^{-7}	3.2073×10^{-7}	3.9108×10^{-7}	3.902×10^{-7}	2.2844×10^{-7}
Rel. E., $N = 20$	1.1235×10^{-9}	1.1377×10^{-9}	1.15×10^{-9}	1.0026×10^{-9}	1.116×10^{-9}
Abs. E., $N = 30$	2.1913×10^{-7}	3.1878×10^{-7}	3.8859×10^{-7}	3.8767×10^{-7}	2.2505×10^{-7}
Rel. E., $N = 30$	1.1159×10^{-9}	1.1308×10^{-9}	1.1427×10^{-9}	9.9612×10^{-10}	1.0995×10^{-9}

Table 2: Errors compared to exact solution for different discretization (into one, two and three shapes) of the wedge

	One Shape	Two Shapes (a)	Two Shapes (b)	Three Shapes
Abs. Error, $N = 20$	3.1141×10^{-7}	3.9526×10^{-7}	4.2335×10^{-7}	4.4145×10^{-7}
Rel. Error, $N = 20$	7.4762×10^{-10}	7.5984×10^{-10}	7.4942×10^{-10}	7.0897×10^{-10}
Abs. Error, $N = 30$	2.7613×10^{-7}	3.8484×10^{-7}	3.892×10^{-7}	4.3211×10^{-7}
Rel. Error, $N = 30$	7.5178×10^{-10}	7.4375×10^{-10}	7.5061×10^{-10}	6.9683×10^{-10}

multishape, can be applied. The exact solution is [4]

$$\rho = \exp(\alpha t + \beta_1 y_1 + \beta_2 y_2)$$

$$\mathbf{v} = \left(\beta_1 - \frac{\alpha}{2\beta_1} + p_1 \exp(-\beta_1 y_1), \beta_2 - \frac{\alpha}{2\beta_2} + p_2 \exp(-\beta_2 y_2) \right),$$

where $\beta_1 = 0.1$, $\beta_2 = 0.1$, $\alpha = -0.5$, $p_1 = -1$ and $p_2 = 1$. We compare the exact solution on a box of dimensions $[0, 2] \times [0, 2]$ with different discretizations of the box using multishape, see Figure 2. Each of the shapes are discretized with $N = 20$ and $N = 30$ points in each spatial direction, which means that the dissected box has more points in total than the original box. The ODE solver tolerances are 10^{-9} . The solution can be seen in Figure 3. The question is whether the results of the PDE on the box and the different discretizations of the box have a similar error when compared to the exact solution. The absolute and relative errors are measured in an L_2 norm in space and an L_∞ norm in time and are displayed in Table 1. The leftmost column contains errors for the non-rectangular quadrilateral, which is shown in Figure 4.

The same test can be done for a wedge. Here, a single wedge and discretized versions are considered, see Figure 5. Table 2 shows the errors measured against the exact solution for different discretizations of the wedge for $N = 20$ and $N = 30$. The solution can be seen in Figure 6.

Next the advection diffusion equation is solved on a multishape which is composed of four

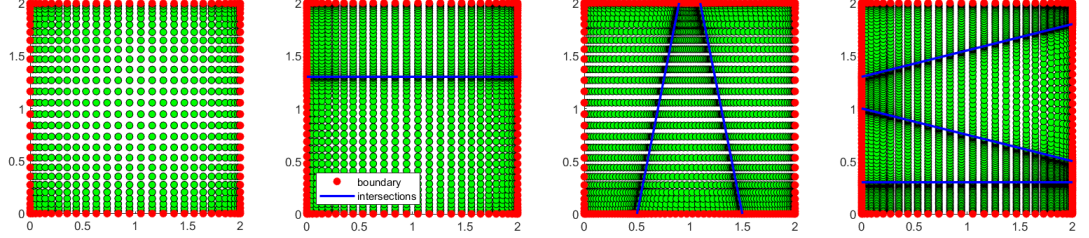


Figure 2: Different discretizations of the box.

quadrilaterals, see Figure 7. The absolute error for $N = 20$ on each shape as compared to the exact solution is 6.1246×10^{-7} and the relative error is 1.3259×10^{-9} . The same is done for a second example involving a wedge, see Figure 8. The absolute error to the exact solution is 3.7239×10^{-7} and the relative error is 8.9375×10^{-10} , when choosing $N = 20$ per shape.

2 Forward Problems on multishapes

We first consider a forward problem on the different discretizations of the box, see Figure 2. We compare the error of the discretizations to the first box without discretization. We choose the initial condition for ρ to be

$$\rho_0 = \exp(-2((y_1 - 0.7)^2 + (y_2 - 0.2)^2))$$

and impose a constant flow of strength 0.8 acting upward. We choose $N = 20$ and $N = 30$ as before. The errors are displayed in Table 3 and the result can be seen in Figure 9.

We follow the same idea, but now consider the wedge discretizations, see Figure 5. We choose the initial condition for ρ to be

$$\rho_0 = \exp(-2((y_1 - 1.5)^2 + (y_2 - 4.5)^2))$$

and impose a constant flow of strength 3 acting from left to right, along the angular direction. We choose $N = 20$ and $N = 30$. The errors are displayed in Table 4 and the result can be seen in Figure 10.

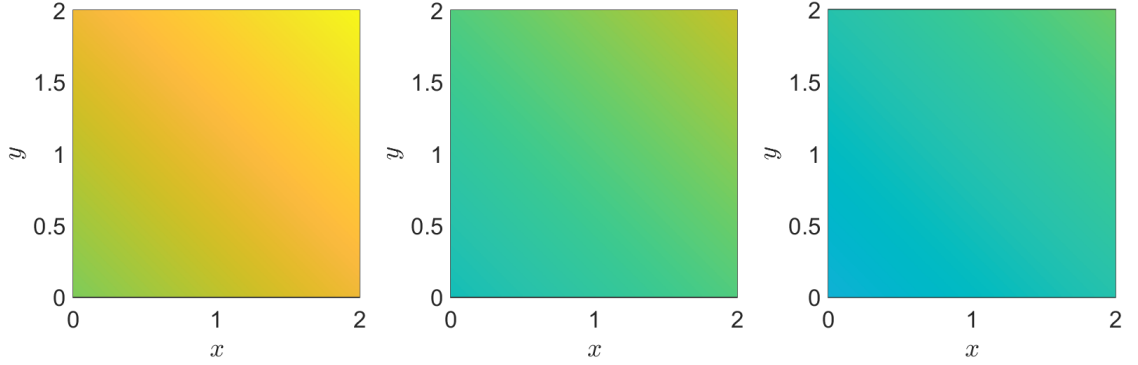


Figure 3: Exact solution on the box.

Table 3: Errors (compared to whole box) for different discretization (into two, three and four shapes) of the box

	Two Shapes	Three Shapes	Four Shapes
Abs. Error, $N = 20$	0.0197	0.0039	0.01
Rel. Error, $N = 20$	0.0015	0.0005	0.0007
Abs. Error, $N = 30$	0.0103	0.0021	0.0053
Rel. Error, $N = 30$	0.0005	0.0002	0.0002

Finally, two multishape examples are shown, which are of interesting shapes. The first of these examples is solving an advection diffusion problem on a multishape consisting of two quadrilaterals and two wedges, with constant velocity of strength ten. The initial condition for this problem is:

$$\rho_0 = \exp(-2(y_1 - 0.5)^2 - 2(y_2 + 1)^2).$$

The result, evaluated for $N = 20$ on each shape, can be seen in Figure 11.

In a second example, the velocity is of strength 5 and the initial condition is:

$$\rho_0 = \exp(-2(y_1 - 0.5)^2 - 2(y_2 - 1.5)^2).$$

The result, which is computed on a multishape made up of four quadrilaterals into a channel, can be seen in Figure 12.

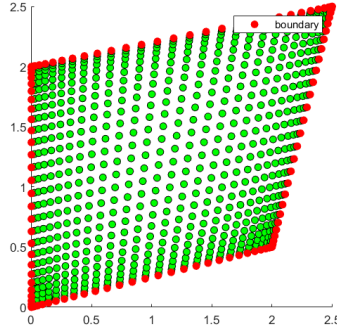


Figure 4: Quadrilateral domain.

Table 4: Errors (compared to whole wedge) for different discretization (into two and three shapes) of the wedge

	Two Shapes (a)	Two Shapes (b)	Three Shapes
Abs. Error, $N = 20$	0.0386	0.0076	0.0693
Rel. Error, $N = 20$	0.0044	0.0007	0.0047
Abs. Error, $N = 30$	0.0215	0.004	0.0383
Rel. Error, $N = 30$	0.0016	0.0002	0.0017

References

- [1] Andreas Nold, Benjamin D. Goddard, Peter Yatsyshin, Nikos Savva, and Serafim Kalliadasis. Pseudospectral methods for density functional theory in bounded and unbounded domains. *CoRR*, abs/1701.06182, 2017.
- [2] Anthony T Patera. A spectral element method for fluid dynamics: Laminar flow in a channel expansion. *Journal of Computational Physics*, 54(3):468–488, 1984.
- [3] Dimitri Komatitsch and Jean-Pierre Vilotte. The spectral element method: an efficient tool to simulate the seismic response of 2d and 3d geological structures. *Bulletin of the Seismological Society of America*, 88:368–392, 04 1998.
- [4] G D Hutomo, J Kusuma, A Ribal, A G Mahie, and N Aris. Numerical solution of 2-d advection-diffusion equation with variable coefficient using du-fort frankel method. *Journal of Physics: Conference Series*, 1180:012009, feb 2019.

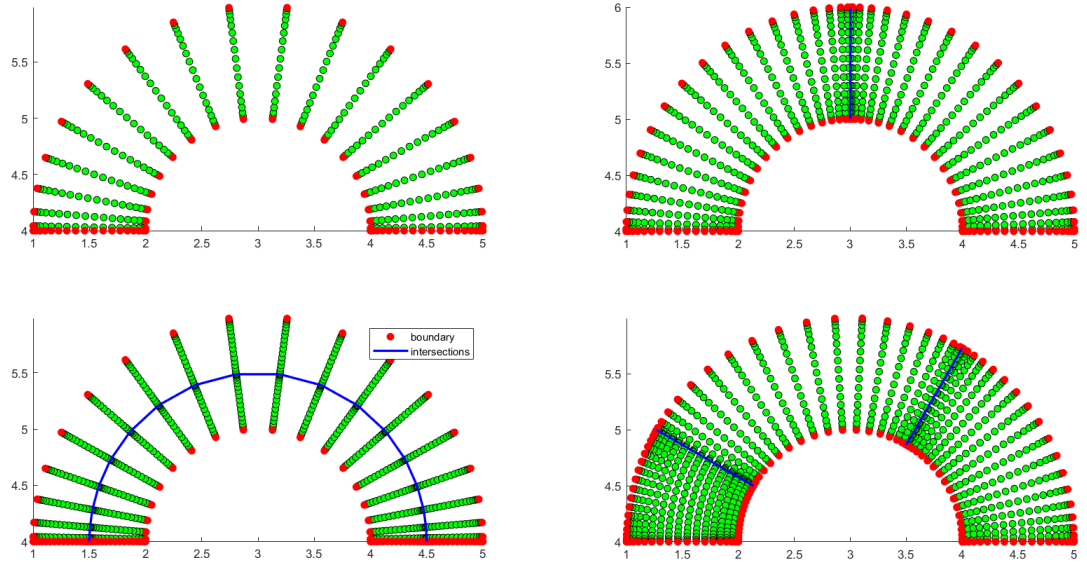


Figure 5: Different discretizations of the wedge.

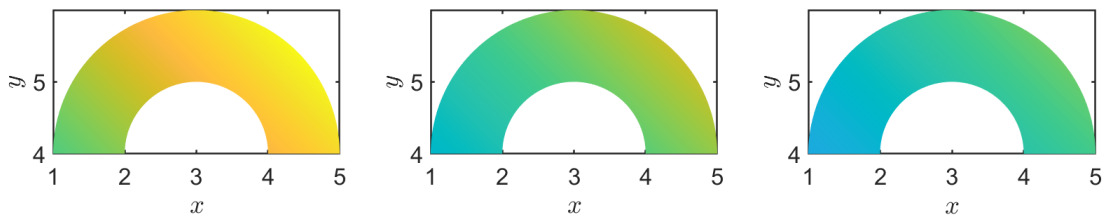


Figure 6: Exact solution on the wedge.

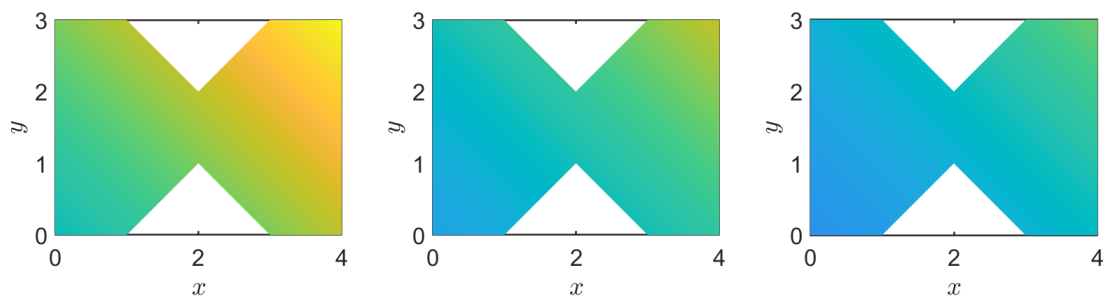


Figure 7: Example 1 multishape

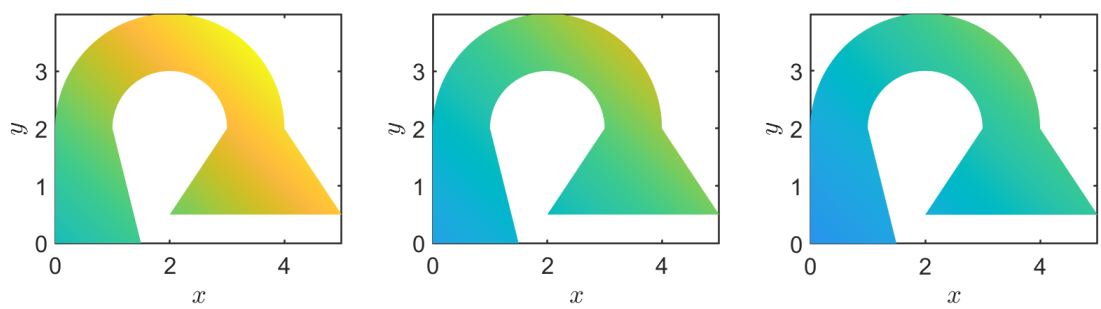


Figure 8: Example 2 multishape

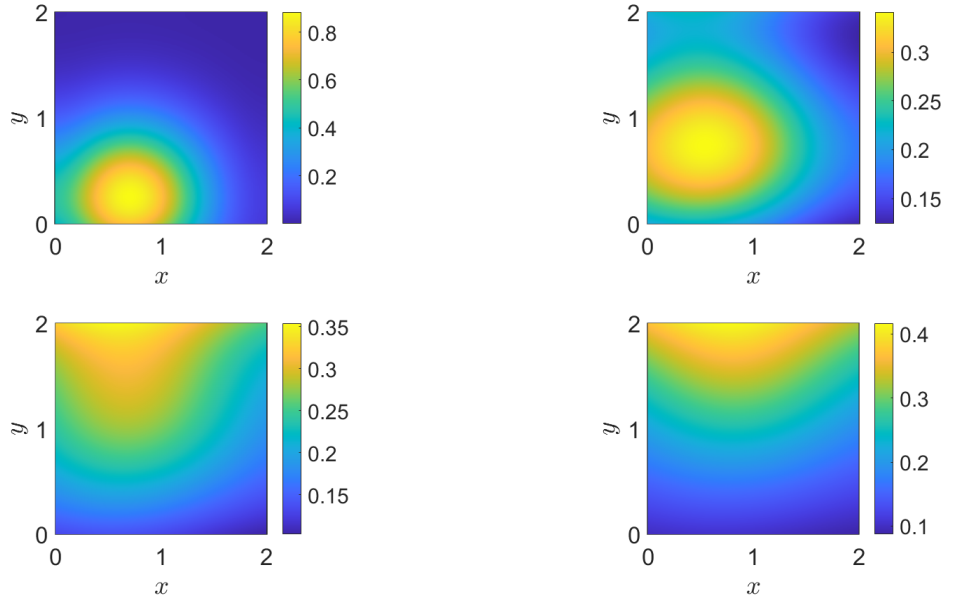


Figure 9: Forward Example on box discretizations

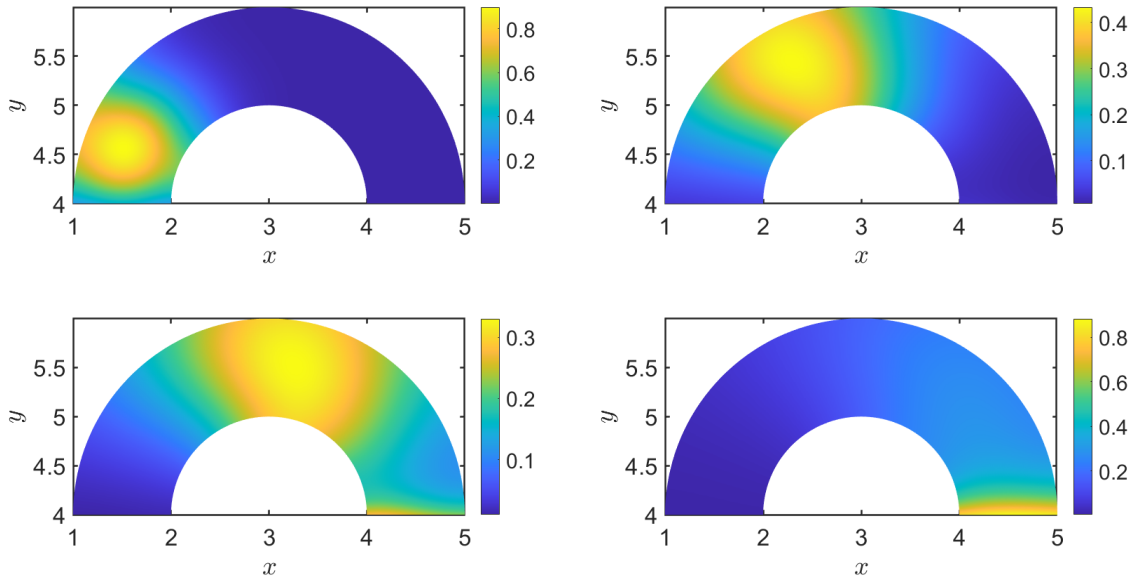


Figure 10: Forward Example on wedge discretizations

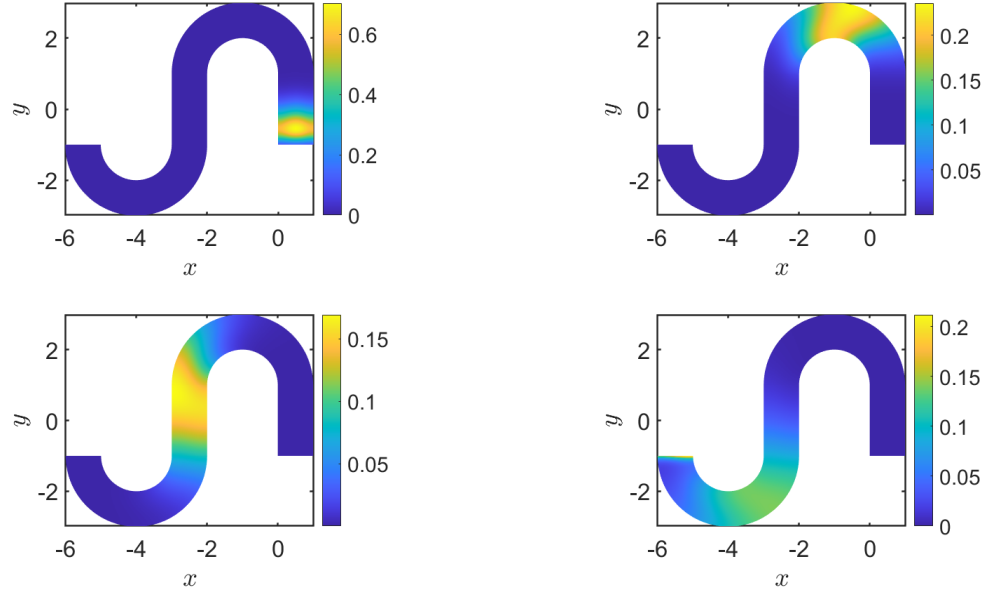


Figure 11: Forward Problem 1, different colour scale for each plot to highlight particle mass location

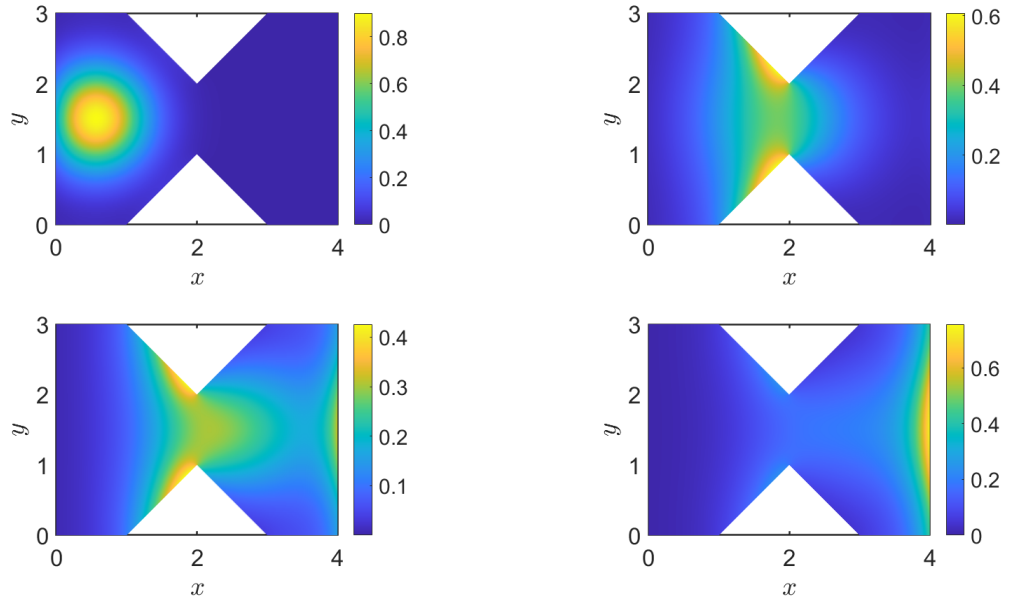


Figure 12: Forward Problem 2, different colour scale for each plot to highlight particle mass location